MULTIPHASE LAYERING AND MOBILITY OF SUSPENDED FINE SEDIMENT IN LAKE APOPKA, FLORIDA

ASHISH J. MEHTA[1], JOHN M. JAEGER[2], ZIYNET BOZ[3] & YOGESH P. KHARE[4]
[1]Department of Civil and Coastal Engineering, University of Florida, Gainesville, Florida, USA.
[2]Department of Geological Sciences, University of Florida, Gainesville, Florida, USA.
[3]Department of Agricultural & Biological Engineering, University of Florida, Gainesville, Florida, USA.
[4]Everglades Foundation, Palmetto Bay, Florida, USA.

ABSTRACT

Fine-grained sediment in Florida's eutrophic lakes displays a characteristically multiphase and layered structure including fluid mud that accounts for most of the nutrient-rich suspended matter potentially contributing to water quality degradation. The viscometric properties of fluid mud layer are particularly important for calculating the sediment load and rate of accumulation. Following a description of fine-sediment layering, a method is outlined to determine the yield stress and viscosity of the characteristically viscoplastic fluid mud. Based upon previous analytic work, these two quantities are deduced from the flow curves for sediment samples (with a mean organic content of about 63%) collected by coring at four sites in Lake Apopka. The analysis indicates an increase in the yield stress and decrease in the relative viscosity with increasing floc volume fraction. Inherent in these trends is the influence of organic content that increases with the floc volume fraction. Comparison with flow curves for sediment of higher density, greater cohesion and lower organic content from a bayou in Louisiana reveals three orders of magnitude higher yield stresses and somewhat lower viscosities relative to Apopka. High yield stresses in the bayou are associated with a dense bed subject to tidal current, which possibly prevents the retention of weak sediment at the bottom. Calculation of the sediment load and annual rate of accumulation due to a fluid mud undercurrent is illustrated for viscous flow over a mildly sloping bottom. For a realistic assessment of the accumulation it will be essential to take into account the role of the episodic wind field and the turbulent flow driving the suspended matter in the lake.
Keywords: bayou, fluid mud, organic sediment, phase change, trophic state, viscosity, yield stress

1 INTRODUCTION

Organic-rich suspended fine sediment particles (≤ 62.5 μm) can be a source of nutrients as well as contaminants. Such sediment has accumulated over the past century in Florida's shallow (1–5 m deep) lakes, and in several instances its presence has led to high trophic states [1]. The need for restoration of water quality due to this problem has provided the impetus to examine sediment dynamics in these lakes as a means to understanding its impact on aquatic biota.

The present focus is Lake Apopka in central Florida, which until about 1947 was mesotrophic with clear water and extensive submersed plant beds [2]. The subsequent degradation of the ecosystem from excessive phosphorus loading persisted until the end of the last century. Management efforts since 1985 have focused on reducing phosphorus loading by the cessation of farming and by restoration of the aquatic system. The water quality has subsequently shown improvement, as indicated by reductions in total phosphorus, chlorophyll and suspended sediment concentration as well as an increase in water transparency and re-appearance of native submersed plants. However, a thick layer of easily resuspended fine-grained muck rich in organic matter and nutrients persists at the bottom.

In what follows, the characteristically stratified multiphase layering of fine sedimentary matter is identified in generic terms. From the point of view of suspended sediment load, the most important layer is the commonly present fluid mud [3]. The two significant variables

ISSN: 2046-0546 (paper format), ISSN: 2046-0554 (online), http://www.witpress.com/journals
DOI: 10.2495/CMEM-V6-N2-433-445

characterizing its transport by gravity over a sloping bed as well as by wind-driven circulation are the viscoplastic yield stress and the dynamic viscosity. Here, a previously reported analytic approach has been recapped and used to determine these two quantities. The utility of the approach for calculating the sediment load is illustrated in terms of viscous flow over a mildly sloping bed.

2 SEDIMENT STRATIFICATION

Figure 1 shows stratified sediment layers in water over a bed consisting of previously deposited and flocculated, or organically aggregated, particles. Let ρ be the wet bulk density of the mixture of sediment and water, ρ_w the water density and ρ_s the material density. Sediment concentration is specified by the volume fraction

$$\phi = \frac{C}{\rho_s} = \frac{\rho - \rho_w}{\rho_s - \rho_w} = \frac{\Delta\rho}{\Delta\rho_s} \tag{1}$$

where C is the dry sediment concentration (e.g. kg m^{-3}). The floc volume fraction ϕ_f is obtained from

$$\phi_f = \frac{\Delta\rho_s}{\Delta\rho_f}\phi \tag{2}$$

where $\Delta\rho_f = \rho_f - \rho_w$ and ρ_f is the floc density. Setting $\phi_f = 1$ in eqn. (2) defines the so-called space-filling volume fraction $\phi_{sp} = \Delta\rho_f / \Delta\rho_s$. Therefore,

$$\phi_f = \frac{\phi}{\phi_{sp}} \tag{3}$$

When ϕ_f is less than 1, the mixture of sediment and water is a suspension in which ephemeral inter-particle bonds can form and break. At the bed surface, defined by $\phi_f = 1$, a phase change occurs from fluid to solid inasmuch as below the bed surface the bonds form an incipient solid-phase, albeit weak, matrix of permanently interconnected particles. With increasing depth in the bed the yield strength of the matrix increases along with ϕ_f [4].

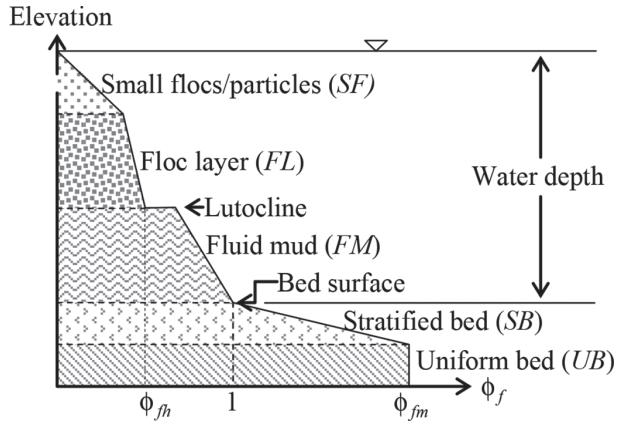

Figure 1: Multiphase, layered fine-grained sediment structure in the aquatic environment.

The fluid mud layer (*FM*) occurs between $\phi_f = 1$ and ϕ_{fh}; the latter quantity represents the onset of hindered settling starting at the lutocline, i.e. the density surface between *FL* and *FM* at which ϕ_f increases significantly. In this mode of settling, particles at high concentration cause settling to be slow as it is controlled by the upward escape of the interstitial fluid (water). In general, *FM* is a transitory state of mud sustained by the kinetic energy of turbulent flow, which may be substantially damped within fluid mud. If energy supply were reduced due to hindered settling, the thickness of *FM* would decrease by self-weight compression and its density (volume fraction) would increase. As a result, close to the bottom of *FM*, mud denser than $\phi_f = 1$ would phase-change to a bed. If, on the other hand, energy supply were to increase, *FM* would dilate as water would be entrained downward into *FM*. Hence, starting from the top of *FM* its density, or ϕ_f, would decrease below ϕ_{fh} and *FM* would gradually change into a dilute suspension (*FL*) in which settling is not hindered. These processes due to changing energy input may render the thickness of *FM* self-preserving during normally (i.e. non-episodically) fluctuating winds, and may explain why in many lakes *FM* tends to be 5–20 cm thick, and much less commonly greater than 30–40 cm [5].

Above *FL* there may be a very dilute suspension, *SF,* containing small flocs, microflocs and colloids which may not deposit readily. Under normal conditions *FL* is sometimes called 'wash load' whose volume fraction may remain more or less invariant. Below *FM* the bed consists of two layers. The increase in ϕ_f with depth in the upper layer (*SB*) is the outcome of consolidation. In the lower, relatively uniform layer *UB,* the maximum floc volume fraction ϕ_{fm} is achieved under self-weight (consolidation). Further compression (over-consolidation) of the bed due to a high surcharge (overburden) may further increase the volume fraction [4].

In *FM* the viscoplastic mud is defined by the yield stress τ_{y0} and the dynamic viscosity η. The following description sets up the physical basis for the determination of these two variables.

3 FLOW CURVE REPRESENTATION

Figure 2 shows the viscoplastic flow curve, i.e. the relationship between shear stress τ and shear strain rate $\dot{\gamma}$ in a compliant fine sediment sample. Its thixotropic behavior is shear-thinning (with a decrease in the curve slope, or viscosity η, as $\dot{\gamma}$ increases) and encloses a loop formed by the rising and falling arms of the flow curve. Starting with the plastic yield stress τ_{y0} at $\dot{\gamma} = 0$, the rising arm is obtained by applying a low stress τ (or $\dot{\gamma}$) over a preselected duration Δt, and then increasing τ (or $\dot{\gamma}$) in steps of the same duration. After the maximum

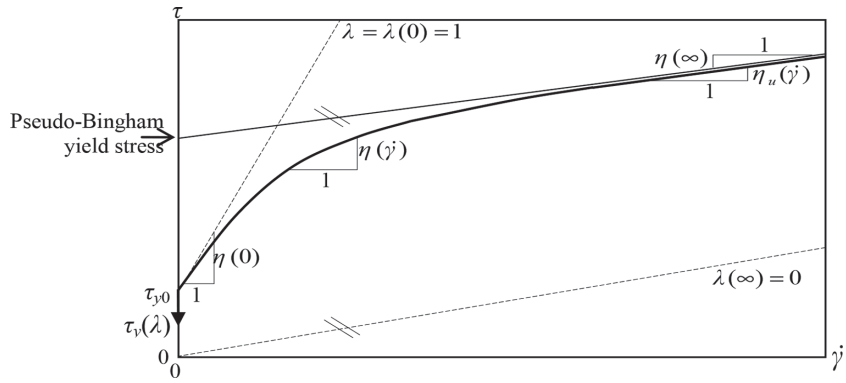

Figure 2: Shear-thinning viscoplastic flow curve.

τ is applied the falling curve is obtained by decreasing τ in the reverse order. The rising and falling loci will trace a single equilibrium curve provided Δt is long enough to achieve equilibrium at a given τ (or $\dot{\gamma}$). Typically, as Δt is selected in tests to be too short for equilibrium, at a given equilibrium stress (τ_e) the strain rate $\dot{\gamma}_R$ of the rising curve is smaller than the equilibrium value $\dot{\gamma}_e$ and, conversely, $\dot{\gamma}_F$ during the falling curve is larger than $\dot{\gamma}_e$ Thus, Δt determines the gap between the rising and falling curves.

Another influential factor is aging, which causes the viscosity of the freshly prepared sample to increase until a duration T (hours, days, weeks …). When $T >> \Delta t$, or when $T << \Delta t$, aging does not interfere in the establishment of equilibrium as it would if $T \approx \Delta t$, in which case equilibrium can be achieved only after the sample is fully aged. In general, upon starting a test, shearing irreversibly breaks down (but does not necessarily deflocculate) the initially intact structure. Resting (hence aging) the sample rebuilds the structure. A characteristic feature of the equilibrium curve is the so-called bottom bend over which the decrease in η with increasing $\dot{\gamma}$ is rapid. With a further increase in $\dot{\gamma}$ the curve slope approaches the constant viscosity of a Newtonian fluid.

To explain the equilibrium curve, $\tau_e = f(\dot{\gamma}_e)$, Moore [6] introduced the notion of a time-dependent structure-related parameter $\lambda(t)$ representing the instantaneous fraction of inter-particle bonds in the sample. Referring to Fig. 3, when τ_e is equal to or less than τ_{y0} and $\dot{\gamma}$ is 0, $\lambda = \lambda(0)$ represents a fully formed structure. This in turn permits an arbitrary assignment of $\lambda(0)$ as (its maximum value) 1. As $\dot{\gamma}$ approaches ∞ the structure breaks down, i.e. λ approaches 0, and the fluid viscosity $\eta(\dot{\gamma})$ tends to the characteristically constant Newtonian value $\eta(\infty)$. The so-called pseudo-Bingham yield stress of a shear-thinning material defined by the asymptotic Bingham viscoplastic line is larger than τ_{y0}. Observe also that the line λ = 0 is parallel to the Bingham line. As $\dot{\gamma}$ increases above 0, the yield stress $\tau_y(\lambda)$, which is intrinsic to the structure (hence not readily measurable), decreases from τ_{y0} to 0 (Newtonian fluid). This allows us to conveniently define λ as

$$\lambda = \frac{\tau_y(\lambda)}{\tau_{y0}} \tag{4}$$

The general viscoplastic equation of the equilibrium flow curve is

$$\tau_e = \eta(\dot{\gamma}, \lambda_e)\dot{\gamma} + \tau_y(\lambda) \tag{5}$$

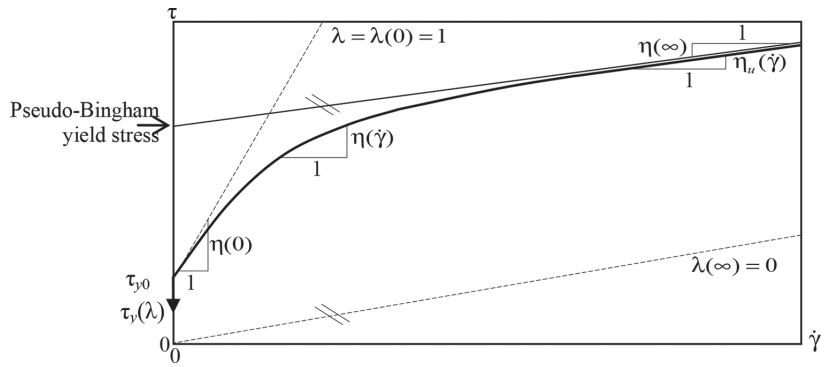

Figure 3: Representation of structure parameter and yield stress.

From an inspection of experimental data on flocculated clay samples, Warrall and Tuliani [7] selected the viscosity function

$$\eta(\dot{\gamma}, \lambda_e) = \eta_u(\dot{\gamma}) + c\lambda_e \tag{6}$$

where the viscosity $\eta_u(\dot{\gamma})$ is such that $\eta_u(\infty) = \eta(\infty)$. Furthermore, $c = \eta(0) - \eta(\infty)$, and $\eta(0)$ is the initial viscosity (Fig. 3). Thus, making use of eqn. (4) we obtain

$$\tau = \left[\eta_u(\dot{\gamma}) + c\lambda_e\right]\dot{\gamma} + \lambda\tau_{y0} \tag{7}$$

In eqn. (7), λ_e and $\eta_u(\dot{\gamma})$ must be replaced by measurable variables. To that end we note that λ, a dynamic quantity, is determined by the rates of growth and breakup of the structure, i.e. from the balance

$$\frac{d\lambda}{dt} = \text{Rate of growth of structure - rate of breakup of structure} \tag{8}$$

We will consider these rates as first-order processes [7], although higher-order representations can be considered, if necessary. The growth rate is taken to be proportional to the instantaneous anomaly between $\lambda(0)$ and λ, i.e.

$$\text{Growth rate} = k_a\left[\lambda(0) - \lambda\right] \tag{9}$$

where k_a is a rate constant. As for breakup

$$\text{Breakup rate} = -k_b\dot{\gamma}\lambda \tag{10}$$

where k_b is another rate constant. Therefore,

$$\frac{d\lambda}{dt} = k_a\left[\lambda(0) - \lambda\right] - k_b\dot{\gamma}\lambda \tag{11}$$

Along the equilibrium flow curve $d\lambda/dt = 0$, hence we get the equilibrium value of λ from

$$\lambda_e = \frac{\lambda(0)}{1 + \left(\dfrac{k_a}{k_b}\right)\dot{\gamma}} \tag{12}$$

As expected, starting with $\lambda(0)$ (= 1) at $\dot{\gamma} = 0$, λ_e decreases with increasing $\dot{\gamma}$ and is 0 when $\dot{\gamma} \to \infty$. Substitution of eqn. (12) into (11) gives

$$\frac{d\lambda}{dt} = -(k_b + k_a\dot{\gamma})\left(\lambda - \lambda_e\right) \tag{13}$$

which indicates that the rate of change of λ is proportional to λ-λ_e.

Finally, substitution of eqn. (12) into (7) gives

$$\tau = \left[\eta_u(\dot{\gamma}) + \frac{c\lambda(0)}{1 + \left(\dfrac{k_a}{k_b}\right)\dot{\gamma}}\right]\dot{\gamma} + \lambda(t)\tau_{y0} \tag{14}$$

which is valid for the first-order rate eqn. (13).

To evaluate $\eta_u(\dot{\gamma})$ consider eqn. (7) for the equilibrium flow curve

$$\tau_e = \left[\eta_u(\dot{\gamma}) + c\lambda_e\right]\dot{\gamma} + \lambda_e\tau_{y0} \tag{15}$$

Relative to this we note that from their experimental measurements Worrall and Tuliani [7] independently stated the equilibrium flow curve as

$$\tau_e = \left[\eta(\infty) + c\lambda_e\right]\dot{\gamma} + \lambda(0)\tau_{y0} \tag{16}$$

The multiplier $\lambda(0)$ has been added for mathematical convenience; it has no bearing on the yield stress because its value is 1. From eqns. (15) and (16)

$$\eta_u(\dot{\gamma})\dot{\gamma} = \eta(\infty)\dot{\gamma} + \left[\lambda(0) - \lambda_e\right]\tau_{y0} \tag{17}$$

Upon substitution of eqn. (17) into (7) we get

$$\tau = \left[\eta(\infty) + c\lambda_e\right]\dot{\gamma} + \left[\lambda_0 - \lambda_e + \lambda(t)\right]\tau_{y0} \tag{18}$$

This general flow curve equation derived by Toorman [8] is valid for any form of eqn. (8). For the equilibrium flow curve, eqn. (18) reduces to

$$\tau = \left[\eta(\infty) + c\lambda_e\right]\dot{\gamma} + \lambda(0)\tau_{y0} \tag{19}$$

For a first-order rate equation, substituting eqn. (12) into this equation gives, with $\lambda(0) = 1$,

$$\tau = \eta(\infty)\dot{\gamma} + \frac{c\dot{\gamma}}{1 + \left(\dfrac{k_a}{k_b}\right)\dot{\gamma}} + \tau_{y0} \tag{20}$$

which was also obtained independently by Worrall and Tuliani [7] but from a less rigorous analysis than that of Toorman [8]. Observe that the second term within the brackets accounts for the bottom bend. The viscosity $\eta(\dot{\gamma})$ is obtained from

$$\eta(\dot{\gamma}) = \frac{d\tau}{d\dot{\gamma}} = \eta(\infty) + \frac{c}{\left[1 + \left(\dfrac{k_a}{k_b}\right)\dot{\gamma}\right]^2} \tag{21}$$

This relationship indicates a characteristically decreasing excess viscosity η-$\eta(\infty)$ with increasing $\dot{\gamma}$ commonly represented empirically by a power-law decay function [9]. Values of $\eta(\infty)$ (approximated as the high-end slope of the measured flow curve) and τ_{y0} are read off from the curve, $c = \eta(0)$-$\eta(\infty)$ and k_a/k_b is determined by tuning.

4 TESTS AND RESULTS

Lake Apopka (Fig. 4) has a surface area of about 12,500 ha and a maximum depth of about 2.5 m relative to the mean sea level datum. Three freshwater springs feed the lake, while the Apopka-Beauclair Canal with a flow-control structure is the only outlet. The organic matter (*OC*) in the bottom sediment ranges between 50% and 70% by weight with a mean of about 63%. Biogenic silica is an important constituent of the non-cohesive mineral sediment. As a result of their low buoyant weight the primarily bio-aggregated particles are easily resuspended at moderate wind speeds [2].

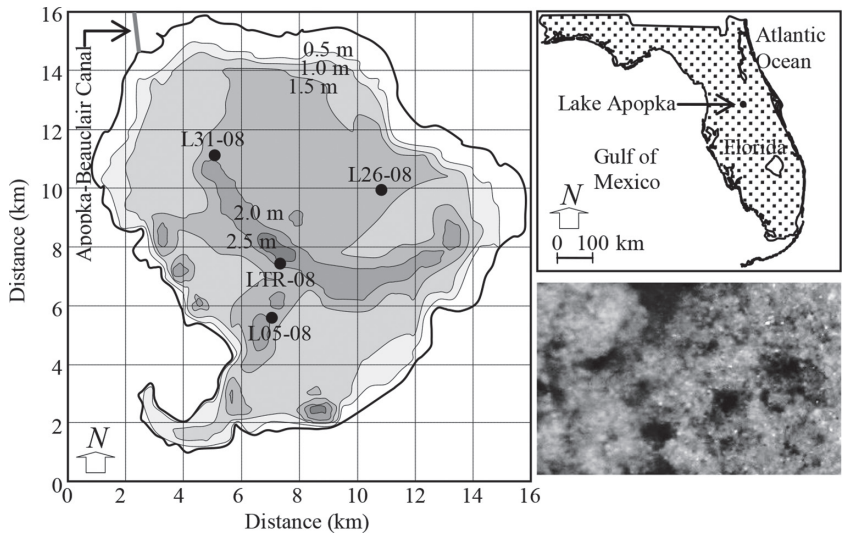

Figure 4: Lake Apopka Florida (FL) water depths (relative to mean sea level) and core sites. Aggregates forming fluid mud are 2–3 mm in diameter.

As part of a field campaign to document the properties of bottom sediment and its resuspension, four sampling stations were cored in 2008 (Fig. 4). Sediment density (hence ϕ) was determined gravimetrically as well as by gamma-ray attenuation [10]. A Brookfield LVDV-I Prime digital applied-strain-rate viscometer with a rotating bob was used to obtain the flow curves at shear strain rates $\dot{\gamma}$ of 1 s^{-1} and less. This value represents the typical non-episodic flow shear in the lake. For measurements, 100 ml samples were extruded from the cores, and each sample was gently stirred so as not to disaggregate them just prior to viscometric testing at 22 °C. At the beginning of the test $\dot{\gamma}$ was set to a minimum value ($5x10^{-3}$ s^{-1}) and increased to 1 s^{-1} in Δt = 10 min steps. Following this, $\dot{\gamma}$ was reduced down to the minimum in the reverse steps. After these tests, *OC* (loss of weight by ignition) was determined in the laboratory [10].

Based on measurements using the full-length (up to 0.4 m) cores LTR-08, L05-08 and L26-08, Fig. 5 suggests a roughly exponential decrease in ϕ as the mineral sediment is

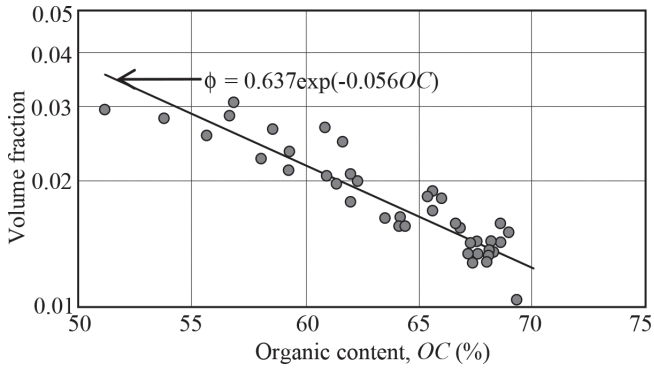

Figure 5: Variation in volume fraction with organic content; Lake Apopka sediment.

increasingly replaced by the lighter organic matter. Based on the space-filling volume fraction ϕ_{sp} found from separate hindered settling tests on the sediment to be 0.019 (revised from [11]), the data are observed to include fluid mud as well as soft bed sediment. Referring to the flow curves, values of ϕ, OC, and the parameters τ_{y0}, $\eta(\infty)$, c and k_a/k_b are given in Table 1 for eight Apopka samples, all being fluid mud. For each of the four cores the first sample was the approximately 3.5-cm-long topmost segment and the second was the next lower segment of about the same length. As examples, two sets of equilibrium flow curve data (obtained by averaging the rising and falling arms; Fig. 2) and eqn. (20) are shown in Fig. 6.

Included in Table 1 for comparison are analogous values for bottom sediment samples A-01 through A-07 collected by coring in 2014 along the cross-section of a shallow tidal

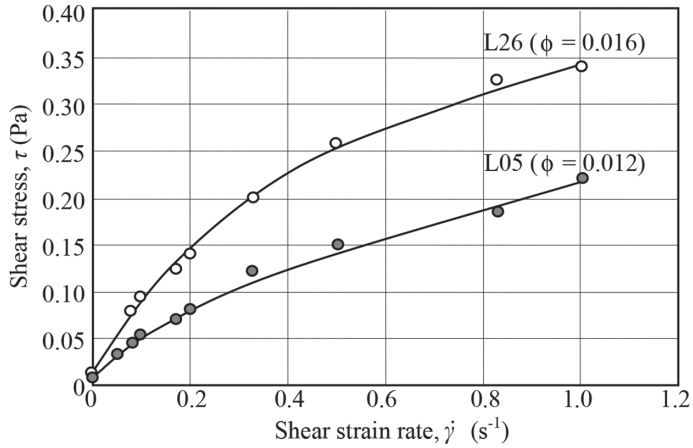

Figure 6: Example flow curves – data points and eqn. (20) curves for Lake Apopka samples.

Table 1: Properties and flow curve parameters Apopka (FL) and bayou (LA) samples

No.	Sample	ϕ	OC (%)	τ_y (Pa)	$\eta(\infty)$ (Pa.s)	c	k_a/k_b
1	LTR-08, FL	0.015	64.5	5.000E-02	1.469E-01	8.000E-01	0.350
2	LTR-08, FL	0.015	63.5	4.000E-02	3.000E-02	6.500E-01	0.350
3	L-05, FL	0.017	65.2	3.500E-02	1.000E-01	7.000E-01	0.370
4	L-05, FL	0.014	63.5	2.000E-02	7.000E-02	7.500E-01	0.370
5	L-26, FL	0.012	62.8	2.000E-02	5.000E-04	1.692E-01	0.570
6	L-26, FL	0.012	61.2	1.000E-02	1.000E-02	3.938E-01	0.570
7	L-31, FL	0.016	63.9	1.500E-02	5.000E-02	9.000E-01	0.330
8	L-31, FL	0.013	63.5	3.000E-02	7.500E-02	6.000E-01	0.330
9	A-01, LA	0.469	41.0	4.000E+01	1.000E+00	1.900E+02	0.410
10	A-02, LA	0.351	44.0	8.000E+01	1.000E-01	1.000E+02	0.670
11	A-03, LA	0.300	50.0	1.590E+02	1.000E-02	3.146E+01	0.900
12	A-04, LA	0.437	33.0	7.500E+01	1.000E-02	2.200E+02	0.225
13	A-05, LA	0.419	30.0	1.500E+02	5.000E-03	2.000E+02	0.185
14	A-06, LA	0.412	24.0	8.000E+01	1.000E-03	1.800E+02	0.330
15	A-07, LA	0.444	25.0	1.081E+02	1.000E-02	5.000E+01	0.270

creek (bayou) in Louisiana (LA). The mean *OC* of the samples was about 35%, which is substantially lower than in Lake Apopka. Due to this and the presence of clays (of unknown mineralogy), flocculation was mainly electrochemical, although floc properties are believed to have been influenced by long-chain (exopolymeric) binding. Sediment characterization and viscometric tests (in a Brookfield DV-II+Pro programmable viscometer with HA7, 0.125 cm dia., spindle) were procedurally similar to those for the Apopka samples [12].

In Fig. 7a, the yield stress of Apopka samples is plotted against ϕ_f with the recognition that the rheological properties of flocculated/aggregated sediment are better represented by the floc volume fraction in preference to ϕ [9]. The yield stress is observed to increase rapidly with ϕ_f. In contrast, it can be observed in Fig. 7b that the viscosity relative to water, $\eta(\infty)/\eta_w$, decreases rapidly with ϕ_f. These (approximate) trends suggested by the respective equations in the insets are characteristic of flocculated clays [13]. However, relative to clay flocs the presence of organic matter and its variation with the volume fraction (Fig. 5) implies a complex interaction between yield stress, viscosity and concentration of the suspended matter. Moreover, aggregation of Apopka sediment was expectedly governed by exopolymers. The lack of well-behaved trends (in Figs. 7a and 7b the r^2 values are 0.22 and 0.45, respectively) are likely to be due to vertical and lateral inhomogeneity in the composition of the lake deposit formed by episodic events in earlier years [11]. Another source of scatter in Fig. 7b possibly arises from the termination of the tests at fairly low shear strain rates (1 s^{-1}) because the main purpose of the original investigation [10] was for the measurement of yield stress (not viscosity). As a consequence, the values of $\eta(\infty)$ possibly do not represent the (expectedly lower) Newtonian values at high rates of shear strain.

Illustrative flow curves of the bayou sediment (Table 1) in Fig. 8 indicate yield stresses three orders of magnitude higher (mean value of seven samples 98.9 Pa) and somewhat lower relative viscosity (6.03×10^{-5} Pa.s) compared to Apopka (0.275 Pa and 1.62×10^{-4} Pa.s, respectively). These substantial differences in the yield stress are believed to be due to: (1) as mentioned, the bayou bottom was subject to strong tidal currents which expectedly prevented the deposition of weak erodible sediment. Thus the bottom was much denser with the consistency of a 'soft' bed rather than fluid mud (the mean value of ϕ was 0.41 as opposed to 0.014

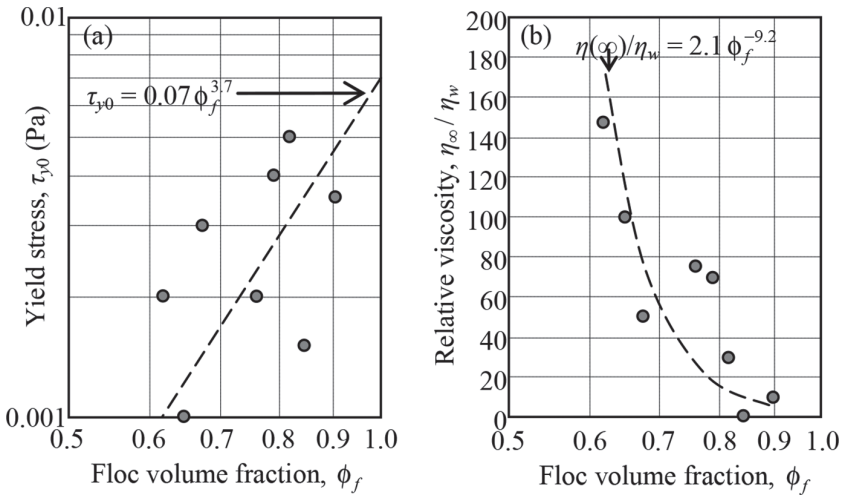

Figure 7: (a) Yield stress and (b) relative viscosity versus ϕ_f; Lake Apopka samples.

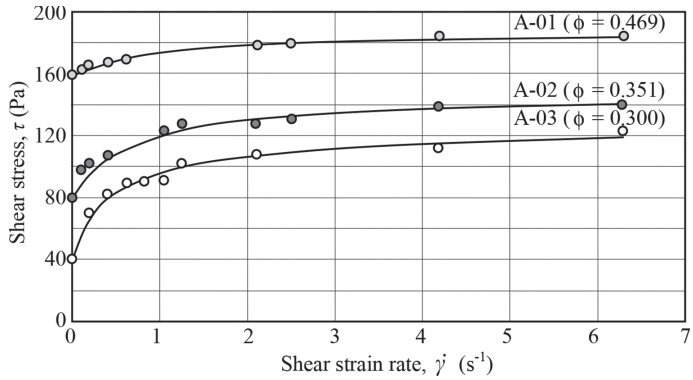

Figure 8: Data points and eqn. (20) curves for bayou samples.

at Apopka). (2) The clayey sediment was highly cohesive in contrast to the organic-rich sediment in Apopka. (3) As indicated, flow curve data at higher shear strain rates were not obtained for the Apopka samples, which was possibly the most significant reason for the high values of $\eta(\infty)/\eta_w$ of Apopka samples. It follows that the application of eqn. (20) along with the best-fit parameters is limited to the maximum shear train rate on the order of 1 s^{-1}. Thus the derived fluid mud viscosities are relevant to typical wind conditions but not to high winds.

5 FLUID MUD MOBILITY

In lakes where mobile fluid mud may disperse contaminants, a conceivable approach to contain the mobile suspended matter is by designating trenches as traps from which accumulated sediment can be taken out. Figure 9 can be referred to estimate the rate of accumulation, in which x and z are the distance coordinates along the flow direction and perpendicular to flow, respectively, and θ is the bed slope (angle). We will illustrate a hypothetical case of purely gravity flow of fluid mud undercurrent over a mildly sloping bottom. It is desired to calculate the mean flow velocity U and the unit dry sediment load g_{ss} (dry mass flux per unit time per unit width of flow).

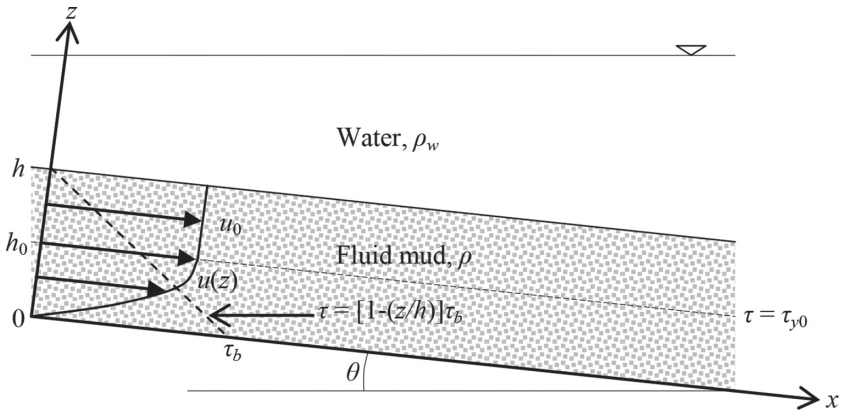

Figure 9: Fluid mud layer moving downslope.

The thickness of fluid mud (*FM* in Fig. 1) is $h(x)$ and its uniform wet bulk density is ρ [see eqn. (1)]. The flow is so slow that it is reasonable to consider it to be viscous. At a height h_0, the shear stress profile assumed to be invariant in the x-direction intersects the $\tau = \tau_{y0}$ plane. Above this plane the fluid has a constant un-sheared flow velocity u_0 and below the plane the boundary layer profile is $u(z)$. Neglecting flow acceleration, the equation of motion can be stated as

$$\frac{\partial \tau}{\partial z} + g\Delta\rho \sin\theta - g\frac{\partial h\Delta\rho}{\partial x}\cos\theta = 0 \tag{22}$$

where $\Delta\rho = \rho - \rho_w$. Considering the interfacial shear stress at h_0 due to the sliding of *FM* relative to water above to be negligible, the shear stress profile is given by

$$\tau = \left(1 - \frac{z}{h}\right)\tau_b; \quad \tau_b = gh\Delta\rho\cos\theta\left(\tan\theta - \frac{\partial h}{\partial x}\right) \tag{23}$$

where τ_b is the bed shear stress. The simplest form of eqn. (5), the Bingham equation (line in Fig. 3), can be conveniently stated as [9]

$$\tau = \tau_{y0} + \eta(\infty)\dot{\gamma} = \tau_{y0} + \eta(\infty)\frac{\partial u}{\partial z}; \quad \tau \geq \tau_{y0} \text{ and } \eta(\infty)\dot{\gamma} = \eta(\infty)\frac{\partial u}{\partial z} = 0; \quad \tau < \tau_{y0} \tag{24}$$

After combining eqns. (22) and (24) and integrating we obtain the velocity profile (see [14] for complete derivation)

$$u = \begin{cases} \dfrac{\tau_b h}{2\eta(\infty)}\left[2\zeta\left(\dfrac{z}{h}\right) - \left(\dfrac{z}{h}\right)^2\right]; & 0 < \dfrac{z}{h} < \zeta \\ = u_0 = \dfrac{\tau_b h}{2\eta(\infty)}\zeta^2; & \zeta < \dfrac{z}{h} < 1 \end{cases} \tag{25}$$

where $\zeta = z / h_0$. Thus, as at $z = h_0$ the stress $\tau = \tau_{y0}$, we obtain $\zeta = 1 - (\tau_{y0} / \tau_b)$. The mean velocity U is now obtained from eqn. (25) as

$$U = \frac{1}{h}\int_0^h u dz = \frac{\tau_b h}{2\eta(\infty)}\zeta^2\left(1 - \frac{\zeta}{3}\right) \tag{26}$$

Finally, the unit sediment load is

$$g_{ss} = \rho_s \phi U \tag{27}$$

Based on eqn. (21) let us consider $\eta(1)$ at 1 s^{-1} as the representative viscosity. From Table 1 the mean value of $\eta(1)$ for the Apopka samples is 0.391 Pa.s. Further, select the following quantities: ρ_s = 1,873 kg m^{-3} [11], dry sediment concentration C = 5 kg m^{-3} of moving fluid mud typical to the lake yielding $\phi = 2.67\text{x}10^{-3}$, $\tau_{y0} = 10^{-4}$ Pa (fluid mud with very low yield strength), h = 0.05 m (a thin near-bed layer of fluid mud), $\theta = 0.0115^o$ (corresponding to a nominal, lake-scale bottom gradient of 1:5000; Fig. 4) and ρ_w = 1,000 kg m^{-3} [15]. From eqn. (1) we obtain $\Delta\rho = \phi\Delta\rho_s$ = 2.33 kg m^{-3}, and ignoring the contribution of the water head $\partial h/\partial x$ to τ_b in eqn. (23), $\tau_b = gh\Delta\rho\sin\theta = 2.29\text{x}10^{-4}$ Pa. Therefore, $\zeta = 0.564$, $U = 3.79\text{x}10^{-6}$ m s^{-1} and $g_{ss} = 1.90\text{x}10^{-5}$ kg m^{-2} s^{-1}, or 598 kg m^{-2} yr^{-1}.

6 CONCLUDING COMMENTS

The above 'textbook' example shows that low strength, organic-rich mud can be mobile even over a nearly horizontal bed. In such an environment one would expect the bottom to be even. To some extent this is evident from Fig. 4, which indicates that in much of the lake the depth range is 1–2 m relative to mean sea level datum, i.e. lake-scale slopes (e.g. 0.0115°) are small.

The calculations are constrained by two assumptions: (1) viscous flow regime and (2) gravity-driven fluid mud undercurrent. The first assumption is satisfied as the Reynolds number $\mathrm{Re} = \rho hU/\eta$ is a very low 3.86×10^{-6}. In reality, fluid mud is generated mainly by wind-driven flows, which assume considerable importance under episodic winds and associated turbulence [15]. The characteristic entrainment of water by turbulent gravity current is not amenable to analytic development and requires numerical hydrodynamic simulation [14].

ACKNOWLEDGMENTS

The authors acknowledge support from the St. Johns River Water Management District, Palatka, Florida, for the field investigation of Lake Apopka. Thanks are due to Jeremy Spearman of HR Wallingford, UK, for his review of a draft. Bayou samples were provided by William H. McAnally of Dynamic Solutions LLC, Knoxville TN.

REFERENCES

[1] Chung, E.G., Bombardelli, F.A. & Schladow, S.G., Modeling linkages between sediment resuspension and water quality in a shallow, eutrophic, wind-exposed lake. *Ecological Modelling*, **220**, pp. 1251–1265, 2009. https://doi.org/10.1016/j.ecolmodel.2009.01.038

[2] Coveney, M.F., Lowe, E.F., Battoe, L.E., Marzolf, E.R. & Conrow, R., Response of a shallow, eutrophic subtropical lake to reduced nutrient loading. *Freshwater Biology*, **50**, pp. 1718–1730, 2005. https://doi.org/10.1111/j.1365-2427.2005.01435.x

[3] McAnally, W.H., Friedrichs, C., Hamilton, D., Hayter, E., Shrestha, P., Rodriguez, H., Sheremet, A. & Teeter, A., Management of fluid mud in estuaries, bays, and lakes I: present state of understanding on character and behavior. *Journal of Hydraulic Engineering*, **133**, pp. 9–22, 2007. https://doi.org/10.1061(asce)0733-9429(2007)133:1(9)

[4] Reddi, L.N. & Inyang, H.I., *Geoenvironmental engineering: principles and application*, Marcel Dekker, 2000.

[5] Kirby, R., Organic-rich fine sediments in Florida part I: sources & nature. In Maa, J.P.-Y., Sanford, L.P. & Schoellhamer, D.H., eds., *Estuarine and coastal fine sediment dynamics*, Elsevier, pp. 147–166, 2007.

[6] Moore, F., The rheology of ceramic slips and bodies. *Transactions of the British Ceramics Society*, **58**, pp. 470–494, 1959.

[7] Worrall, W.E. & Tuliani, S., Viscosity changes during the aging of clay-water suspensions. *Transactions of the British Ceramic Society*, **63**, pp. 167–185, 1964.

[8] Toorman, E.A., Modeling thixotropic behavior of dense cohesive sediment suspensions. *Rheologica Acta*, **36**, pp. 56–65, 1997. https://doi.org/10.1007/bf00366724

[9] Barnes, H.A., Hutton, J.F. &Walters, K., *An introduction to Rheology*, Elsevier, Chicago, 1989.

[10] Jaeger, J.M. & Ullrich, A., Physical, compositional and rheological properties of Lake Apopka sediment, in: Mehta, A.J., Jaeger, J.M., So, S., Valle–Levinson, A., Hayter, E.J., Wolanski, E. & Manning, A.J. Resuspension dynamics in Lake Apopka, Florida, *Final Report*, St. Johns River Water Management District, Palatka, Florida, Appendix A, 2009.

[11] Mehta, A.J., Hwang, K.-N. & Khare, Y.P., Critical shear stress for mass erosion of organic-rich fine sediments. *Estuarine, Coastal and Shelf Science*, **165**, pp. 97–103, 2015.
https://doi.org/10.1016/j.ecss.2015.08.020

[12] Mehta, A.J., Boz, Z. & Khare, Y.P., *Viscoplastic yield stress and critical shear stress for erosion of mud samples*, unpublished, 2014.

[13] Migniot, C., A study of the physical properties of different very fine sediments and their behavior under hydrodynamic action. *La Houille Blanche*, **7**, pp. 591–620, 1968 (in French, with abstract in English).
https://doi.org/10.1051/lhb/1968041

[14] van Kessel, T. & Kranenburg, C., Gravity current of fluid mud along sloping bed. *Journal of Hydraulic Engineering*, **122**(12), pp. 710–717, 1996.
https://doi.org/10.1061/(asce)0733-9429(1996)122:12(710)

[15] Mehta, A.J. & Hayter, E.J., Effects of some ecohydrological thresholds on the stability of aquatic fine-sediment beds, Wolanski, E. & McLusky, D.S., eds., *Treatise on Estuarine and Coastal Science*, **9**, Academic Press, pp. 425–439, 2011.